Research Square

Preprints are preliminary reports that have not undergone peer review.
They should not be considered conclusive, used to inform clinical practice,
or referenced by the media as validated information.

Slow Afterhyperpolarization as a Neural Mechanism for Allostatic Opponent-Process Dynamics

Nathan I. N. Henry

nathan.henry@uwa.edu.au

University of Western Australia

Mangor Pedersen

Auckland University of Technology

Research Article

Keywords: Allostasis, opponent-process theory, slow afterhyperpolarization, amygdala, spike-frequency adaptation, affective dynamics

Posted Date: June 19th, 2026

DOI: https://doi.org/10.21203/rs.3.rs-9604512/v1

License: This work is licensed under a Creative Commons Attribution 4.0 International License.
Read Full License

Additional Declarations: No competing interests reported.

Abstract

The brain needs to be adaptable to internal and external stimuli for survival. Solomon and Corbit's opponent-process theory, in which the initial response to a stimulus (the "a-process") is followed by an opposite reaction (the "b-process"), provides a temporal framework for the adaptation of affective dynamics in response to stimuli. With repeated stimulation, the a-process diminishes while the b-process strengthens, reflecting an adaptive process known as allostasis. However, the neural mechanisms behind allostasis remain largely unknown. In this simulation study, we modelled the short-term opponent-process of a fear response as the mean-field potential across excitatory neuronal populations in the basolateral amygdala, using Izhikevich neurons to replicate neural firings. We show that modulating parameters of the slow afterhyperpolarization (sAHP) reproduces the characteristic decrease in a-process magnitude and increase in b-process magnitude associated with allostasis, yielding the canonical "standard pattern of affective dynamics". In this framework, the a-process corresponds to the initial depolarization of neural populations, while sAHP dynamics, together with slower processes such as neurotransmitter depletion, account for short- and long-timescale b-processes. These results provide a plausible cellular mechanism for affective allostasis and fear adaptation, and suggest that intrinsic population dynamics provide a biophysical substrate for affective regulation.

Introduction

Biological survival relies on the brain's capacity for allostasis – the maintenance of stability through physiological change (Sterling, 2012). In contrast to homeostasis, in which the brain maintains a physiological system at a fixed set point, allostasis is the process by which internal states are dynamically adapted to match the fluctuating demands of intrinsic and extrinsic stimuli (McEwen & Wingfield, 2003). These adaptive mechanisms are a fundamental biological requirement; without them, neural circuits lack the necessary constraints to prevent persistent stimuli from driving the system into a state of chronic activation, dysregulation, and hyperexcitability (Glei et al., 2007; Hanson & Nacewicz, 2021). However, despite the clear biological necessity of these processes, the mechanisms that coordinate such adaptations remain largely unknown.

One possible solution to this problem lies in opponent-process theory, which describes the affective response to a stimulus as the interplay of a fast, primary "a-process" and a slower, opposing "b-process" that grows in strength with repeated stimulation, producing tolerance, withdrawal, and habituation (Koob & Le Moal, 2008; Solomon & Corbit, 1974). The valence of these processes is oppositional, such that if the a-process is a positive emotion, then the b-process is a negative emotion. With repeated stimuli (for example, in the case of drug tolerance induced by addiction), the b-process increases in magnitude while the a-process decreases – an adaptive mechanism known as allostasis (George et al., 2012; McEwen, 2000). The allostatic opponent-process curve (Fig. 1) has framed our understanding of emotion, drug addiction and sensory habituation for many years (George et al., 2012; Koob & Le Moal, 2008; Solomon &

Corbit, 1974), but remains a purely psychological account, offering no cellular or circuit-level explanation for how the net affective value of a stimulus can invert over time.

Currently, neuroscience-based opponent-process models lack a plausible cellular substrate for producing b-processes associated with negative emotions. Contemporary computational models of affective dynamics, whether based on firing rates or mean-field descriptions of local field potentials (e.g., Buzsáki, 2004; Wilson & Cowan, 1972) capture certain aspects of cognitive dynamics and can explain the weakened a-process, but fail to reproduce the negative rebound required to generate the inverted b-process. Nor do the synaptic-plasticity models of dopamine release (e.g., Berridge & Robinson, 1998; Schultz, 1997) explain the rapid, non-linear rebound seen in short-timescale affective shifts, or capture how neurotransmitter depletion yields long-term withdrawal (Koob & Le Moal, 2008).

Within the brain, a region that has been consistently linked to both positive and negative emotional processing is the amygdala (Ambroggi et al., 2008; Fox et al., 2015; Hanson & Nacewicz, 2021). Some research has attempted to explain opponent-process dynamics within this region. For example, Hagihara & Lüthi (2024) proposed that in the amygdala's intercalated cell (ITC) clusters, the dorsomedial ITC neurons serve as a dedicated system for encoding negative valence (scaling with shock intensity), while the functionally contrasting ventromedial ITC neurons encode positive valence (responding to rewards), together forming a proposed neural substrate for the opponent-process theory of motivation. Still, while such theories may explain a weakened a-process, they do not explain the temporal variations in these processes to the level of precision required to replicate the ‘standard pattern of affective dynamics’ (SPOAD) described in Solomon & Corbit’s paper (1974).

Yet surprisingly, there exists a well-known neural phenomenon that exhibits opponent-process dynamics on a similar timescale to the SPOAD, albeit with a different shape and scale: the action potential. Many neurons fire action potentials with a slow afterhyperpolarization (sAHP) period that resembles the b-process on a similar timescale to that in the SPOAD. However, this mechanism has been overlooked as a source of this phenomenon, perhaps due to the lack of similarity between the shape of the neural opponent-process and that of the emotional opponent-process. For example, the “a-process” of the neural membrane potential is far shorter and more intense than that of the SPOAD. However, this ignores the possibility that aggregated neural population dynamics may provide a different temporal pattern that more closely resembles the traditional pattern of affective dynamics (Henry et al., 2023).

In this article, we propose that the opponent-process is not just a psychological abstraction, but an intrinsic feature of the action potential itself, where a depolarizing a-process (Na^+ influx) is inherently followed by a hyperpolarizing b-process (K^+- and Ca^{2+}-mediated afterhyperpolarization). In the following sections, we will show, via computational modelling of neuron populations, how mean-field membrane-potential trajectories reproduce classical opponent-process dynamics, and how parameter variations in sAHP and neurotransmitter dynamics can replicate b-process allostasis. Consequently, this would allow the mean membrane potential to dip below resting potential, thus encoding negative rebounds (i.e., b-processes) that other mechanisms such as firing rates cannot reproduce.

To validate this theory, we implement our model in a population of simulated Izhikevich neurons within the basolateral amygdala (BLA), chosen due to its well-documented firing patterns and biophysical properties. This work is intended as a testable computational theory that links cellular dynamics to observable affective temporal patterns.

Theory

3.1 Neural firing patterns in the basolateral amygdala

When humans are exposed to aversive stimuli, the majority of neurons in the BLA typically respond by exhibiting regular or tonic spiking with spike frequency adaptation (Faber et al., 2001). These spike trains are followed by a pronounced slow afterhyperpolarization (sAHP), which is mediated by Ca^{2+}-dependent K^+ currents and creates a transient refractory period that reduces neuronal excitability (Andrade et al., 2012). The result is a biphasic voltage trajectory with an initial positive voltage spike, followed by a longer, lower-amplitude opposing voltage spike that, coincidentally, resembles the b-process in the SPOAD.

Faber et al. (2001) showed that the amplitude of the AHP largely explains the firing properties of lateral amygdala (LA) neurons in rats, a sub-component of the BLA. For example, blocking calcium influx with cadmium blocks the sAHP and reduces spike frequency adaptation. Hence, firing frequency is dependent on the magnitude and duration of the sAHP, which in turn is calcium-dependent (Andrade et al., 2012; Faber et al., 2001). This highlights a potential mechanism for allostasis in opponent-process theory: by increasing the magnitude and duration of the sAHP, one could simulate a reduction in the firing frequency and the size of the a-process while simultaneously increasing the size and duration of the b-process.

3.2 Fear responses

In vivo recordings show that fear-encoding neurons in the BLA respond to threatening cues with high-frequency bursts of action potentials that rapidly adapt with repeated exposure (Quirk et al., 1995). In a timescale of several seconds, this adaptation reflects both intrinsic mechanisms such as sAHP and Na^+/K^+-pump-mediated hyperpolarization. However, over longer timescales (minutes to hours), this reflects synaptic factors like vesicle depletion and receptor desensitization (Zucker & Regehr, 2002). Over time, these mechanisms diminish the net excitatory response to repeated stimuli, capturing the tolerance and habituation dynamics central to opponent-process theory.

These firing properties can be reproduced using tonic spiking Izhikevich neurons, parameterized with a strong recovery variable u to capture spike-frequency adaptation and sAHP dynamics. By augmenting the model with an activity-dependent afterhyperpolarization term, the full trajectory of BLA neuron excitability during and after stimulation can be simulated. As we will demonstrate, the mean-field membrane potential $\bar{V}(t)$ derived from these populations naturally reproduces the temporal structure

of the canonical opponent-process curve, including rebound dips, tolerance buildup, and allostatic adaptation following repeated stimulations.

Methods

Neural dynamics were simulated using a modified Izhikevich spiking neuron model (Izhikevich, 2003). We selected this model to balance biological plausibility with the computational efficiency required to simulate large populations. The traditional model was augmented with a third state variable, w, representing an activity-dependent sAHP current applied at spike events. The system is described by the following ordinary differential equations:

$$\mathrm{d}v/\mathrm{d}t = 0.04v^2 + 5v + 140 - u + I_{applied} - w$$

1.

$$\mathrm{d}u/\mathrm{d}t = a\left(bv - u\right)$$

2.

$$\mathrm{d}w/\mathrm{d}t = -w/\tau$$

3.

where v is the membrane potential, u is the membrane recovery variable, and w is the sAHP current. The term $I_{applied}$ represents an externally applied stimulus current. The parameters a, b, c and d are dimensionless constants that determine the neuron's intrinsic firing characteristics, such as tonic spiking or bursting. Upon spike detection ($v \geq$ 30 mV), state variables are reset:

$$v \leftarrow c$$

4.

$$u \leftarrow u + d$$

5.

$$w \leftarrow w + \delta_{AHP}$$

6.

This event-based reset instantaneously repolarizes the membrane potential to a value of c, increments the recovery variable u by a value of d, and increases the AHP current w by a fixed increment, δ_{AHP}. The AHP current w then decays back to zero with a time constant of τ , contributing to spike-frequency adaptation and bursting behaviours. The sAHP current is modelled as a spike-triggered process, where each action potential contributes a fixed increment (δ_{AHP}) that decays exponentially over time, approximating the accumulation of intracellular calcium underlying biological sAHP currents.

While the shape of the post-stimulus hyperpolarization matches that of the SPOAD b-process, the pattern of firing exhibited by individual neurons in Fig. 2 clearly does not match the shape of the SPOAD in Fig. 1. Yet a plot of *spike frequency against time* for a single neuron produces a trace that does, in fact, qualitatively match the adaptation phase of the SPOAD a-process, where the initial peak of firing reduces to reach a steady-state. Thus, if this trace were summed over a population of neurons, we predicted that it would smooth out to closely replicate the opponent-process curve. This can be achieved by taking the mean-field potential across a population of N BLA neurons at time t:

$$\bar{V}(t) = \frac{\sum_{i=1}^{N} V_i(t))}{N}$$

7.

where $V_i(t)$ is the membrane potential of neuron i at time t. This captures the average state of a neuronal population, reflecting its overall electrical activity without tracking each spike event.

To simulate a population of BLA neurons, a global stimulus was applied to a set of N Izhikevich neurons. The parameters of each neuron were slightly modulated by assigning a normally distributed random error to all parameter values for each neuron, ensuring that each neuron exhibited unique firing patterns.

Sensory information can reach the amygdala via a fast thalamo-amygdala pathway, allowing for a rapid assessment of threat. This activity, which can occur within 15 ms of stimulus presentation (Quirk et al., 1995), suggests that neurons in the initial input layers of the amygdala fire with minimal latency. However, as activation propagates from the lateral amygdala to other nuclei, such as the basolateral and central amygdala, sequential neuronal recruitment occurs, introducing temporal delays in the activation of subsequent neuronal layers (Adke et al., 2021; Aukema et al., 2025; Bienvenu et al., 2012; Lee et al., 2017). To capture this combination of rapid onset and variability in response latency, the stimulus onset times for individual neurons were sampled from a skew-logistic distribution well-suited for describing first-passage times in stochastic processes (Balakrishnan, 1991).

With the model specified, we examined its behaviour under stimulation regimes designed to mimic affective responses. First, we demonstrate the emergence of the SPOAD waveform from the population-averaged activity of multiple BLA neurons. We then systematically manipulated the model's parameters to isolate the specific contributions of mechanisms like the sAHP to the overall opponent-process dynamic.

The model's ODEs were solved using the Euler method in C + + and integrated into an R script via the Rcpp and deSolve packages (Eddelbuettel & Francois, 2011; R Core Team, 2022, p. 202; Soetaert et al., 2010). The code for the simulations is available in the Supplementary Materials and on the Open Science Framework (OSF; https://doi.org/10.17605/OSF.IO/5PC4D).

Results

5.1 Emergence of opponent-process dynamics from population activity

We began by simulating the response of a population of 1000 heterogeneous Izhikevich neurons to a single, transient stimulus lasting several seconds. The stimulus evokes a burst of largely asynchronous firing that is densest at the onset and becomes sparser over time, reflecting spike-frequency adaptation within individual neurons (Fig. 3A). When the membrane potentials of all 1000 neurons are averaged to produce the mean-field potential, $\bar{V}(t)$, the resulting trajectory strikingly reproduces the biphasic SPOAD waveform in Fig. 1.

The emergent waveform can be deconstructed into the five characteristic stages of the SPOAD, as described by Solomon and Corbit (1974) and labelled in Panel C:

1. Peak of a-process: The initial sharp rise in $\bar{V}(t)$ is driven by near-synchronous, high-frequency firing across the population before sAHP currents fully activate.
2. Adaptation: The subsequent decay reflects the accumulation of sAHP currents, which oppose the excitatory drive and reduce the average firing rate.
3. Steady state: A dynamic equilibrium is established where the external stimulus is counterbalanced by the aggregated sAHP, maintaining $\bar{V}(t)$ at a stable, elevated plateau.
4. Peak of b-process: Stimulus cessation immediately unmasks the accumulated hyperpolarizing sAHP currents, driving $\bar{V}(t)$ below the mean resting potential.
5. Decay of b-process: The gradual return to baseline follows the relaxation kinetics of the sAHP current as it deactivates across the neuronal population.

These results demonstrate that the fundamental temporal dynamics of opponent-process theory can emerge as a collective property of a neuronal population, without requiring a separate dedicated circuit for the opposing process.

5.2 Modifying slow afterhyperpolarization parameters

To demonstrate how modifying the sAHP can influence the model, we systematically varied the parameters governing the sAHP current in a series of simulations, with the results shown in Fig. 4. Each panel displays the response of a single representative neuron (top) and the resulting mean-field potential from its corresponding population (bottom).

Panel A shows the baseline response, with identical parameters to that analysed in Fig. 3. In Panel B, we increased the sAHP spike increment δ_{AHP}, effectively increasing the contribution of each action potential to the cumulative sAHP. This resulted in faster and more pronounced spike-frequency

adaptation in each neuron. At the population level, this manipulation caused a significant reduction in the amplitude of the a-process and a corresponding increase in the magnitude and duration of the b-process.

Next, we slowed the decay rate of the sAHP current (τ), as shown in Panel C. This prolonged the hyperpolarizing effect of each spike. While this had less of an impact on the a-process, it led to a substantially longer and deeper b-process in the mean-field potential. Finally, combining an increased sAHP increment with a slower decay rate (Panel D) produced an additive effect. This combination yielded the most dramatic transformation of the opponent-process curve: a severely attenuated a-process and a powerful, prolonged b-process. This latter condition provides a compelling analogue of the allostatic process, whereby repeated exposure to a stimulus (which would lead to potentiation of sAHP currents) causes the opposing after-reaction (the b-process) to dominate the affective response.

Discussion

Allostatic adaptation is a core requirement for neural systems to maintain stability amidst a constant flux of internal and external stimuli. Our results show that allostatic adaptation in affective systems may emerge naturally from the collective mean-field membrane potential of neural populations. By calculating the mean-field membrane potential across a population of Izhikevich neurons augmented with sAHP currents, we reproduced Solomon and Corbit's "standard pattern of affective dynamics" (SPOAD) without requiring a separate, dedicated circuit for the b-process. This finding suggests that the opponent-process mechanism is an emergent phenomenon of population dynamics derived from intrinsic cellular properties, rather than a consequence of oppositional neuronal circuits. Unlike firing-rate models (e.g., Buzsáki, 2004; Wilson & Cowan, 1972), our formulation uses the intrinsic biphasic dynamics of the action potential. Ultimately, this approach may provide a formal framework to quantify allostasis in the brain, offering a neurological mechanism for what has previously been a psychological construct.

Implicit in this model is a form of neural scale invariance: the intrinsic opponent-process dynamic of the single action potential (rapid depolarization followed by sAHP) is aggregated to form the macroscopic affective curve. While a single neuron's trace does not match the psychological SPOAD (due to the lack of a steady-state plateau), the SPOAD waveform emerges at the system level. This shift illustrates that affective dynamics are an emergent property of population-level recruitment – a perspective that aligns with network-based approaches in which the behaviour of individual nodes provides limited information about the collective dynamics of the network (Ebitz & Hayden, 2021; Slomowitz et al., 2015; Vyas et al., 2020). Our findings suggest that population-level aggregating mechanisms, such as volume conduction or even ephaptic coupling, may be necessary to transmit and compute these affective signals across BLA circuits.

To our knowledge, no existing computational model reproduces the full SPOAD waveform directly from cellular-level dynamics. However, while sAHP currents are a sufficient mechanism for opponent-process dynamics, they are not necessarily exclusive. Other mechanisms, such as slow inhibition,

neuromodulatory decay, or synaptic depression, may also combine to generate biphasic responses. Our contribution is to show that a single, well-characterized cellular phenomenon is sufficient to reproduce the SPOAD shape. Yet while it may account for short-term opponent-process dynamics (on the order of seconds), it does not account for longer-term opponent-process mechanisms, such as those involved in addiction. Mid-term dynamics (minutes) likely involve synaptic depression via vesicle depletion, while long-term shifts (days), such as chronic withdrawal or allostasis, are likely to correspond to homeostatic plasticity and shifts in ion channel expression (Koob & Le Moal, 2008). A comprehensive account of opponent-process dynamics will therefore require integrating mechanisms across these timescales, with explicit consideration of the temporal domain under study.

While we do not pursue empirical validation here, the theory yields falsifiable predictions that could be evaluated in future electrophysiological work. If the theory is correct, then pharmacologically inhibiting SK channels (which mediate sAHP) or downregulating Na+/K+-ATPase activity should attenuate the magnitude and duration of the b-process without reducing the initial fear response. However, such experiments would need to be precisely calibrated to avoid triggering pathological hyperexcitability or seizures, which would prevent the observation of allostasis. The amygdala is commonly associated with initiation and propagation of seizures, together with neighbouring structures such as the hippocampus as well as the entorhinal and piriform cortex (Aroniadou-Anderjaska et al., 2008). From a neurobiological perspective, this means that the amygdala is vulnerable to neuronal hyperexcitability and hypersynchronicity (Kullmann, 2011). A failure to achieve neuronal allostasis is a plausible explanation contributing to adaptive neural network changes in the presence of epileptogenic activity (Chang et al., 2018). A study by Toprani and Durand (2013) supports this view. They show that a low frequency electrical stimulation to hippocampal pathways – while inducing sAHP and inhibitory post synaptic potential antagonists – reduces hyperpolarisation length and results in higher seizure frequency (Toprani & Durand, 2013).

If subjective affect correlates with mean-field voltage rather than firing rate, this reframes emotional encoding as a distributed, field-based phenomenon. This offers a biophysical correlate for “affective state” that is distinct from localist or firing-rate models. Practically, this predicts that transitions in emotional valence should map onto Local Field Potentials (LFP), rather than simple changes in spike counts. Beyond the amygdala, this theory suggests that there may be opponent-process phenomena in any group of neurons exhibiting a pronounced sAHP. For example, it may be that the sAHP plays a role in the visual bipolar and ganglion cells. These have been demonstrated to exhibit similar opponent-process dynamics to the SPOAD pattern (e.g., see Figures in Ichinose & Habib, 2022; Johnston et al., 2012). Until now, the consensus is that signal intensity for colour was encoded by the firing rate and temporal pattern of neurons in relevant opponent channels, but it is possible that the mean membrane potential contributes to these opponent-process dynamics.

Some limitations must be addressed. Firstly, our current model simulates a population of excitatory neurons, neglecting inhibitory interneurons. The amygdala relies on a tight excitation-inhibition balance, and it is plausible that a delayed inhibitory postsynaptic potential (IPSP) could contribute to the b-

process. However, synaptic inhibition provides a distinct temporal profile that is insufficient to account for the minute-scale kinetics of the b-process. GABAergic IPSPs typically decay on the order of milliseconds (Sallard et al., 2021). Consequently, a “network-only” model relying solely on synaptic feedback would struggle to maintain the prolonged suppression observed in affective withdrawal without requiring unrealistically long synaptic time constants. In contrast, the b-process described in opponent-process theory, and the sAHP currents modelled here, operate on a timescale of seconds to minutes. While circuit-level inhibition appears to determine the immediate timing of the a-process peak, the slow recovery of the sAHP provides a more parsimonious mechanism for the prolonged decay characteristic of the b-process (withdrawal/rebound). Future iterations should incorporate interneurons to determine how fast synaptic inhibition interacts with these slower adaptation currents. Furthermore, we utilized fixed parameters for τ and δ_{AHP} to simulate allostasis, whereas in reality, these parameters are likely to be dynamically regulated by neuromodulators such as acetylcholine. Thus, future work should model these parameters as dynamic variables under neuromodulatory control. These variable parameters should also be tested across a range of computational models, such as the classic Hodgkin–Huxley and integrate-and-fire models (Hodgkin & Huxley, 1952; Lapicque, 1907). However, there is no obvious reason why the core dynamics of our model would not generalize to those settings, since the critical features of each neuron trace are very similar between models.

In conclusion, we have demonstrated that by taking the mean-field potential across a population of neurons in the basolateral amygdala during a fear response, we can computationally replicate the standard pattern of affective dynamics as proposed by Solomon and Corbit in their paper on opponent-process theory. We have therefore found a plausible mechanism for quantifying short-term affective allostasis in the brain. The replication of the SPOAD trace is achieved because the slow afterhyperpolarization current naturally opposes the initial neural depolarization in neurons, serving as a plausible biological substrate of the opposing b-process. Consequently, this measure offers a tractable candidate for the neural basis of affect and a new avenue for interpreting electrophysiological data in affective neuroscience. Such a mapping between mean membrane potentials and affective states offers new theoretical avenues for relating neural population dynamics to subjective affect, and for exploring the nature of allostatic adaptation in the brain.

Declarations

Ethics approval:

This study is a computational/theoretical investigation and does not involve human participants, animals, or identifiable personal data. Therefore, ethical approval was not required.

Conflicts of interest:

The authors have no competing interests to declare that are relevant to the content of this article.

Funding:

No funding was received for conducting this study.

Author Contribution

Nathan Henry: conceptualization, formal analysis, investigation, methodology, software, validation, visualization, writing – original draft, writing – review & editing. Mangor Pedersen: validation, supervision, writing – original draft, writing – review & editing.

Code availability:

All code used in this study is provided in the Supplementary Materials.

References

1. Adke, A. P., Khan, A., Ahn, H. S., Becker, J. J., Wilson, T. D., Valdivia, S., Sugimura, Y. K., Gonzalez, S. M., & Carrasquillo, Y. (2021). Cell-Type Specificity of Neuronal Excitability and Morphology in the Central Amygdala. *eNeuro*, *8*(1). https://doi.org/10.1523/ENEURO.0402-20.2020
2. Ambroggi, F., Ishikawa, A., Fields, H. L., & Nicola, S. M. (2008). Basolateral Amygdala Neurons Facilitate Reward-Seeking Behavior by Exciting Nucleus Accumbens Neurons. *Neuron*, *59*(4), 648–661. https://doi.org/10.1016/j.neuron.2008.07.004
3. Andrade, R., Foehring, R. C., & Tzingounis, A. V. (2012). The calcium-activated slow AHP: Cutting through the Gordian knot. *Frontiers in Cellular Neuroscience*, *6*. https://doi.org/10.3389/fncel.2012.00047
4. Aroniadou-Anderjaska, V., Fritsch, B., Qashu, F., & Braga, M. F. M. (2008). Pathology and Pathophysiology of the Amygdala in Epileptogenesis and Epilepsy. *Epilepsy Research*, *78*(2–3), 102–116. https://doi.org/10.1016/j.eplepsyres.2007.11.011
5. Aukema, R. J., Petrie, G. N., Lau, B. K., Seabrook, L. T., Baglot, S. L., Christianson, J. P., Bains, J. S., Morena, M., Borgland, S. L., & Hill, M. N. (2025). A network of basolateral amygdala projection neurons contributes to stress-induced activation of the hypothalamic-pituitary-adrenal axis. *Science Advances*, *11*(45), eadv3737. https://doi.org/10.1126/sciadv.adv3737
6. Balakrishnan, N. (1991). *Handbook of the Logistic Distribution*. CRC. https://doi.org/10.1201/9781482277098
7. Berridge, K. C., & Robinson, T. E. (1998). What is the role of dopamine in reward: Hedonic impact, reward learning, or incentive salience? *Brain Research Reviews*, *28*(3), 309–369. https://doi.org/10.1016/S0165-0173(98)00019-8

8. Bienvenu, T. C. M., Busti, D., Magill, P. J., Ferraguti, F., & Capogna, M. (2012). Cell-Type-Specific Recruitment of Amygdala Interneurons to Hippocampal Theta Rhythm and Noxious Stimuli In Vivo. *Neuron*, *74*(6), 1059–1074. https://doi.org/10.1016/j.neuron.2012.04.022
9. Buzsáki, G. (2004). Large-scale recording of neuronal ensembles. *Nature Neuroscience*, *7*(5), 446–451. https://doi.org/10.1038/nn1233
10. Chang, W. C., Kudlacek, J., Hlinka, J., Chvojka, J., Hadrava, M., Kumpost, V., Powell, A. D., Janca, R., Maturana, M. I., Karoly, P. J., Freestone, D. R., Cook, M. J., Palus, M., Otahal, J., Jefferys, J. G. R., & Jiruska, P. (2018). Loss of neuronal network resilience precedes seizures and determines the ictogenic nature of interictal synaptic perturbations. *Nature Neuroscience*, *21*(12), 1742–1752. https://doi.org/10.1038/s41593-018-0278-y
11. Ebitz, R. B., & Hayden, B. Y. (2021). The population doctrine in cognitive neuroscience. *Neuron*, *109*(19), 3055–3068. https://doi.org/10.1016/j.neuron.2021.07.011
12. Eddelbuettel, D., & Francois, R. (2011). Rcpp: Seamless R and C + + Integration. *Journal of Statistical Software*, *40*, 1–18. https://doi.org/10.18637/jss.v040.i08
13. Faber, E. S. L., Callister, R. J., & Sah, P. (2001). Morphological and Electrophysiological Properties of Principal Neurons in the Rat Lateral Amygdala In Vitro. *Journal of Neurophysiology*, *85*, 714–723. https://doi.org/10.1152/jn.2001.85.2.714
14. Fox, A. S., Oler, J. A., Tromp, D. P. M., Fudge, J. L., & Kalin, N. H. (2015). Extending the amygdala in theories of threat processing. *Trends in Neurosciences*, *38*(5), 319–329. https://doi.org/10.1016/j.tins.2015.03.002
15. George, O., Le Moal, M., & Koob, G. F. (2012). Allostasis and addiction: Role of the dopamine and corticotropin-releasing factor systems. *Physiology & Behavior Allostasis and Allostatic Load*, *106*(1), 58–64. https://doi.org/10.1016/j.physbeh.2011.11.004
16. Glei, D. A., Goldman, N., Chuang, Y. L., & Weinstein, M. (2007). Do Chronic Stressors Lead to Physiological Dysregulation? Testing the Theory of Allostatic Load. *Biopsychosocial Science and Medicine*, *69*(8), 769. https://doi.org/10.1097/PSY.0b013e318157cba6
17. Hagihara, K. M., & Lüthi, A. (2024). Bidirectional valence coding in amygdala intercalated clusters: A neural substrate for the opponent-process theory of motivation. *Neuroscience Research*, *209*, 28–33. https://doi.org/10.1016/j.neures.2024.07.003
18. Hanson, J. L., & Nacewicz, B. M. (2021). Amygdala Allostasis and Early Life Adversity: Considering Excitotoxicity and Inescapability in the Sequelae of Stress. *Frontiers in Human Neuroscience*, *15*. https://doi.org/10.3389/fnhum.2021.624705
19. Henry, N., Pedersen, M., Williams, M., & Donkin, L. (2023). Behavioral Posology: A Novel Paradigm for Modeling the Healthy Limits of Behaviors. *Advanced Theory and Simulations*, 2300214. https://doi.org/10.1002/adts.202300214
20. Hodgkin, A. L., & Huxley, A. F. (1952). A quantitative description of membrane current and its application to conduction and excitation in nerve. *The Journal of Physiology*, *117*(4), 500–544. https://doi.org/10.1113/jphysiol.1952.sp004764

21. Ichinose, T., & Habib, S. (2022). On and off signaling pathways in the retina and the visual system. *Frontiers in Ophthalmology*, *2*. https://doi.org/10.3389/fopht.2022.989002
22. Izhikevich, E. M. (2003). Simple model of spiking neurons. *IEEE Transactions on Neural Networks*, *14*(6), 1569–1572.
23. Johnston, J., Esposti, F., & Lagnado, L. (2012). Color Vision: Retinal Blues. *Current Biology*, *22*(16), R637–R639. https://doi.org/10.1016/j.cub.2012.07.022
24. Koob, G. F., & Le Moal, M. (2008). Neurobiological mechanisms for opponent motivational processes in addiction. *Philosophical Transactions of the Royal Society B: Biological Sciences*, *363*(1507), 3113–3123. https://doi.org/10.1098/rstb.2008.0094
25. Kullmann, D. M. (2011). What's wrong with the amygdala in temporal lobe epilepsy? *Brain*, *134*(10), 2800–2801. https://doi.org/10.1093/brain/awr246
26. Lapicque, L. (1907). Recherches quantitatives sur l'excitation electrique des nerfs. *J Physiol Pathol Gen*, *9*, 620–635.
27. Lee, S. C., Amir, A., Haufler, D., & Pare, D. (2017). DIFFERENTIAL RECRUITMENT OF COMPETING VALENCE-RELATED AMYGDALA NETWORKS DURING ANXIETY. *Neuron*, *96*(1), 81–88e5. https://doi.org/10.1016/j.neuron.2017.09.002
28. McEwen, B. S. (2000). Allostasis and Allostatic Load: Implications for Neuropsychopharmacology. *Neuropsychopharmacology : Official Publication Of The American College Of Neuropsychopharmacology*, *22*(2), 108–124. https://doi.org/10.1016/S0893-133X(99)00129-3
29. McEwen, B. S., & Wingfield, J. C. (2003). The concept of allostasis in biology and biomedicine. *Hormones and Behavior*, *43*(1), 2–15.
30. Quirk, G. J., Repa, C., & LeDoux, J. E. (1995). Fear conditioning enhances short-latency auditory responses of lateral amygdala neurons: Parallel recordings in the freely behaving rat. *Neuron*, *15*(5), 1029–1039. https://doi.org/10.1016/0896-6273(95)90092-6
31. R Core Team (2022). *R: A Language and Environment for Statistical Computing*. https://www.R-project.org/
32. Sallard, E., Letourneur, D., & Legendre, P. (2021). Electrophysiology of ionotropic GABA receptors. *Cellular and Molecular Life Sciences*, *78*(13), 5341–5370. https://doi.org/10.1007/s00018-021-03846-2
33. Schultz, W. (1997). Dopamine neurons and their role in reward mechanisms. *Current Opinion in Neurobiology*, *7*(2), 191–197. https://doi.org/10.1016/s0959-4388(97)80007-4
34. Slomowitz, E., Styr, B., Vertkin, I., Milshtein-Parush, H., Nelken, I., Slutsky, M., & Slutsky, I. (2015). Interplay between population firing stability and single neuron dynamics in hippocampal networks. *eLife*, *4*, e04378. https://doi.org/10.7554/eLife.04378
35. Soetaert, K., Petzoldt, T., & Setzer, R. W. (2010). Solving Differential Equations in R: Package deSolve. *Journal of Statistical Software*, *33*, 1–25. https://doi.org/10.18637/jss.v033.i09

36. Solomon, R. L., & Corbit, J. D. (1974). An opponent-process theory of motivation: I. Temporal dynamics of affect. *Psychological Review*, *81*(2), 119–145. https://doi.org/10.1037/h0036128
37. Sterling, P. (2012). Allostasis: A model of predictive regulation. *Physiology & Behavior Allostasis and Allostatic Load*, *106*(1), 5–15. https://doi.org/10.1016/j.physbeh.2011.06.004
38. Toprani, S., & Durand, D. M. (2013). Long-lasting hyperpolarization underlies seizure reduction by low frequency deep brain electrical stimulation. *The Journal of Physiology*, *591*(Pt 22), 5765–5790. https://doi.org/10.1113/jphysiol.2013.253757
39. Vyas, S., Golub, M. D., Sussillo, D., & Shenoy, K. V. (2020). Computation Through Neural Population Dynamics. *Annual Review of Neuroscience*, *43*(Volume 43, 2020), 249–275. https://doi.org/10.1146/annurev-neuro-092619-094115
40. Wilson, H. R., & Cowan, J. D. (1972). Excitatory and inhibitory interactions in localized populations of model neurons. *Biophysical Journal*, *12*(1), 1–24. https://doi.org/10.1016/S0006-3495(72)86068-5
41. Zucker, R. S., & Regehr, W. G. (2002). Short-term synaptic plasticity. *Annual Review of Physiology*, *64*, 355–405. https://doi.org/10.1146/annurev.physiol.64.092501.114547

Footnotes

1. To produce a b-process, the voltage must fall below the neuron's equilibrium potential. The sAHP thus provides a plausible explanation for this dip in voltage, assuming that the magnitude of the membrane potential is the key variable, rather than just the spike frequency.

Figures

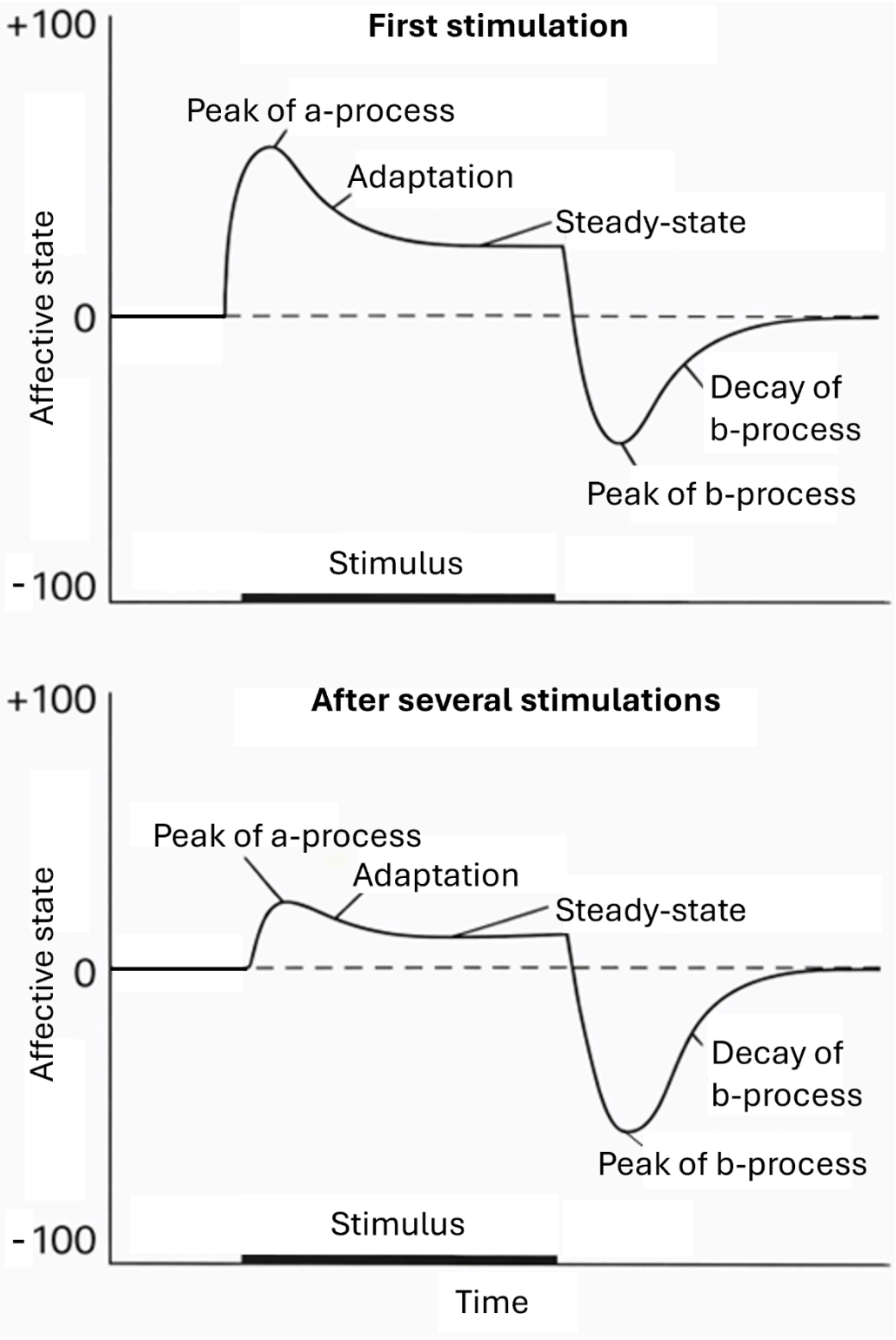


Figure 1

Schematic of the 'standard pattern of affective dynamics' (SPOAD) as proposed by Solomon & Corbit (1974). A single emotional stimulus evokes a fast, positive a-process followed by a delayed, negative b-process. Upon stimulus offset, the b-process dominates briefly before returning to baseline. Repeated or sustained exposure leads to an earlier onset and increased magnitude of the b-process, modelling tolerance, withdrawal, and habituation.

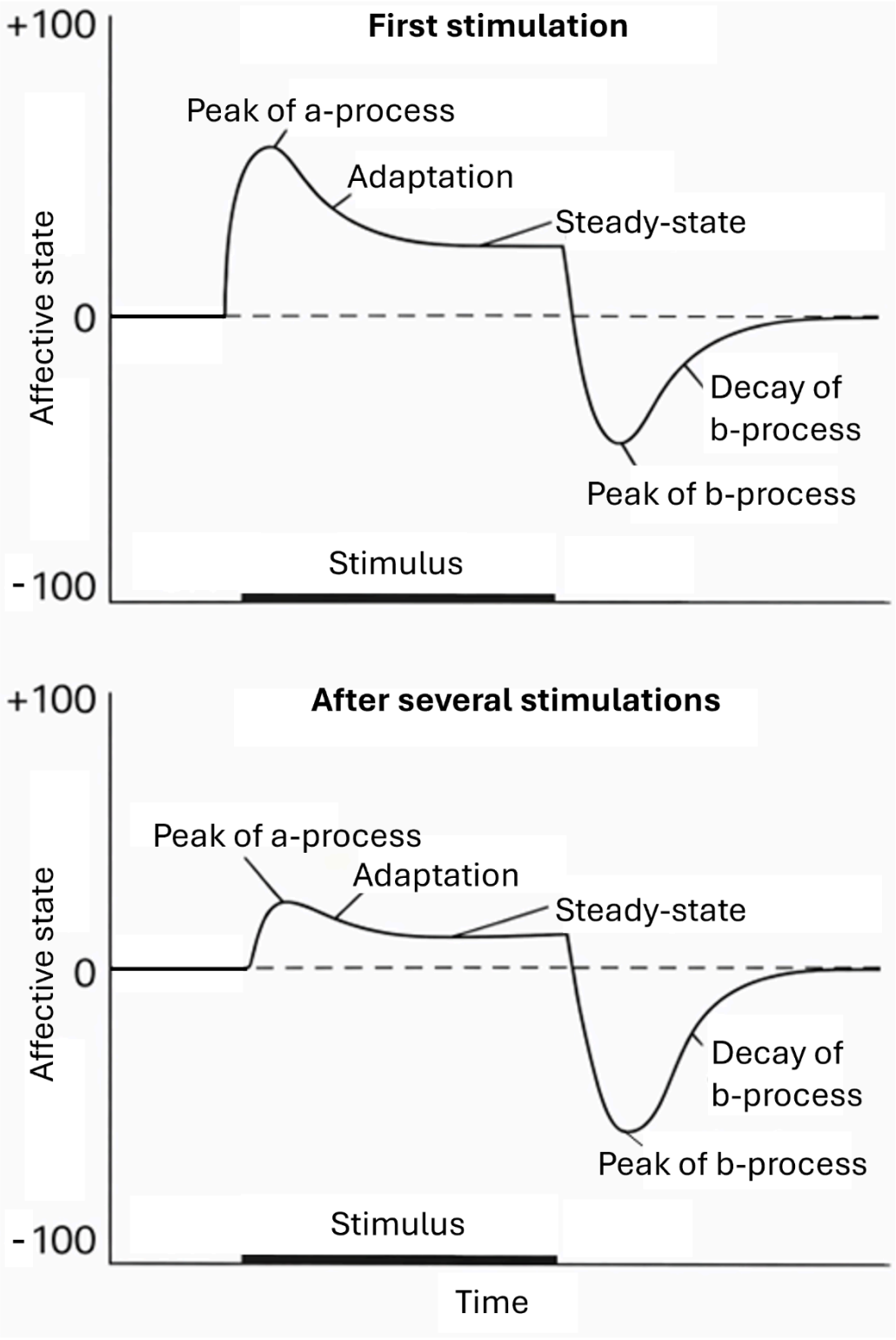


Figure 1

Schematic of the 'standard pattern of affective dynamics' (SPOAD) as proposed by Solomon & Corbit (1974). A single emotional stimulus evokes a fast, positive a-process followed by a delayed, negative b-process. Upon stimulus offset, the b-process dominates briefly before returning to baseline. Repeated or sustained exposure leads to an earlier onset and increased magnitude of the b-process, modelling tolerance, withdrawal, and habituation.

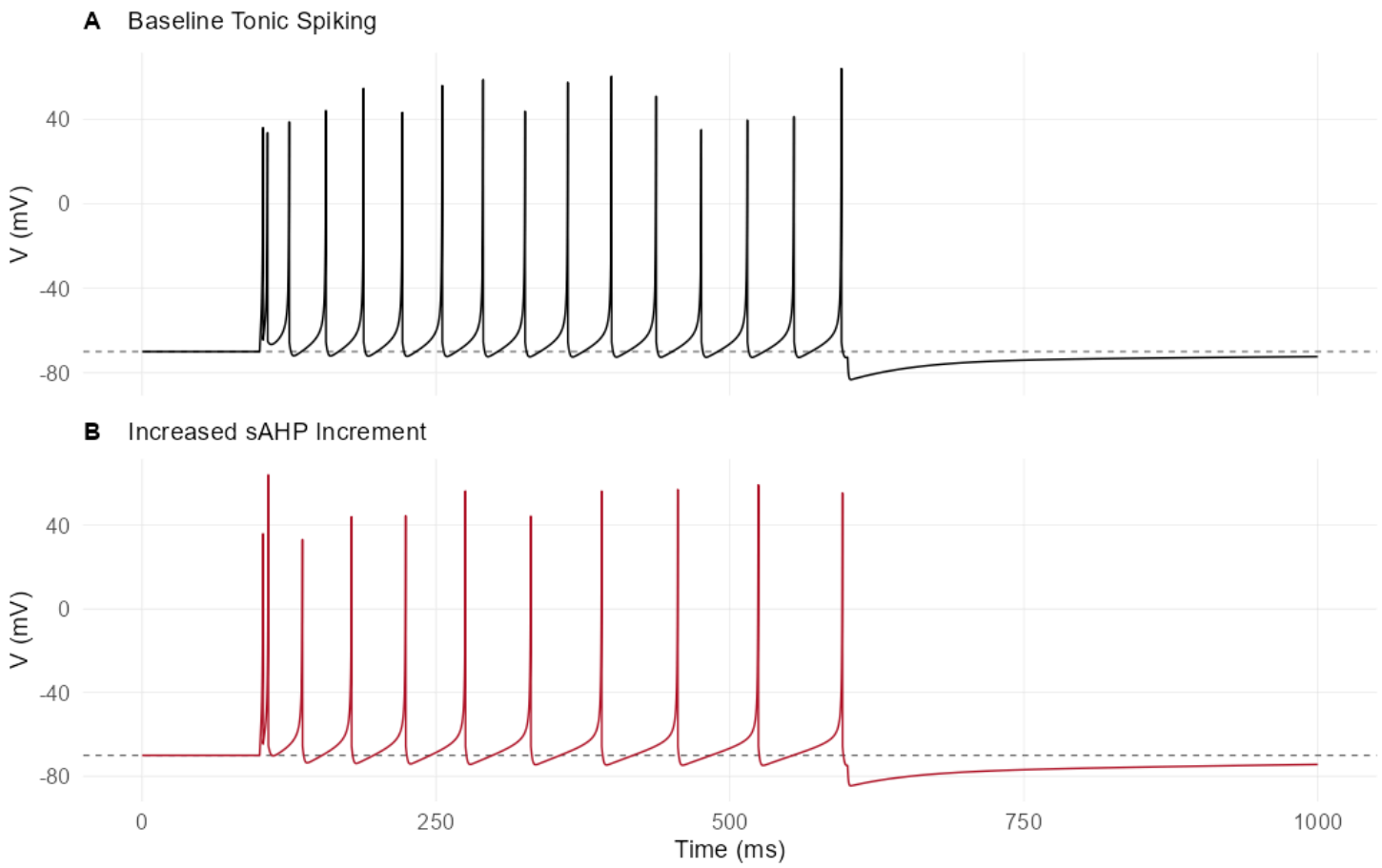


Figure 2

Single-neuron simulations showing how the sAHP modulates firing in an Izhikevich model. Stimulus is applied continuously from 100 to 600 ms. (A) Control neuron without sAHP current applied shows sustained spiking throughout stimulus duration. (B) Application of a stronger sAHP hastens adaptation during stimulation, dramatically reducing spike frequency and producing a more pronounced hyperpolarization once the stimulus is turned off. Both simulations use identical input currents and stimulus durations; sAHP strength is modulated by varying the sAHP decay and increment per spike parameters.

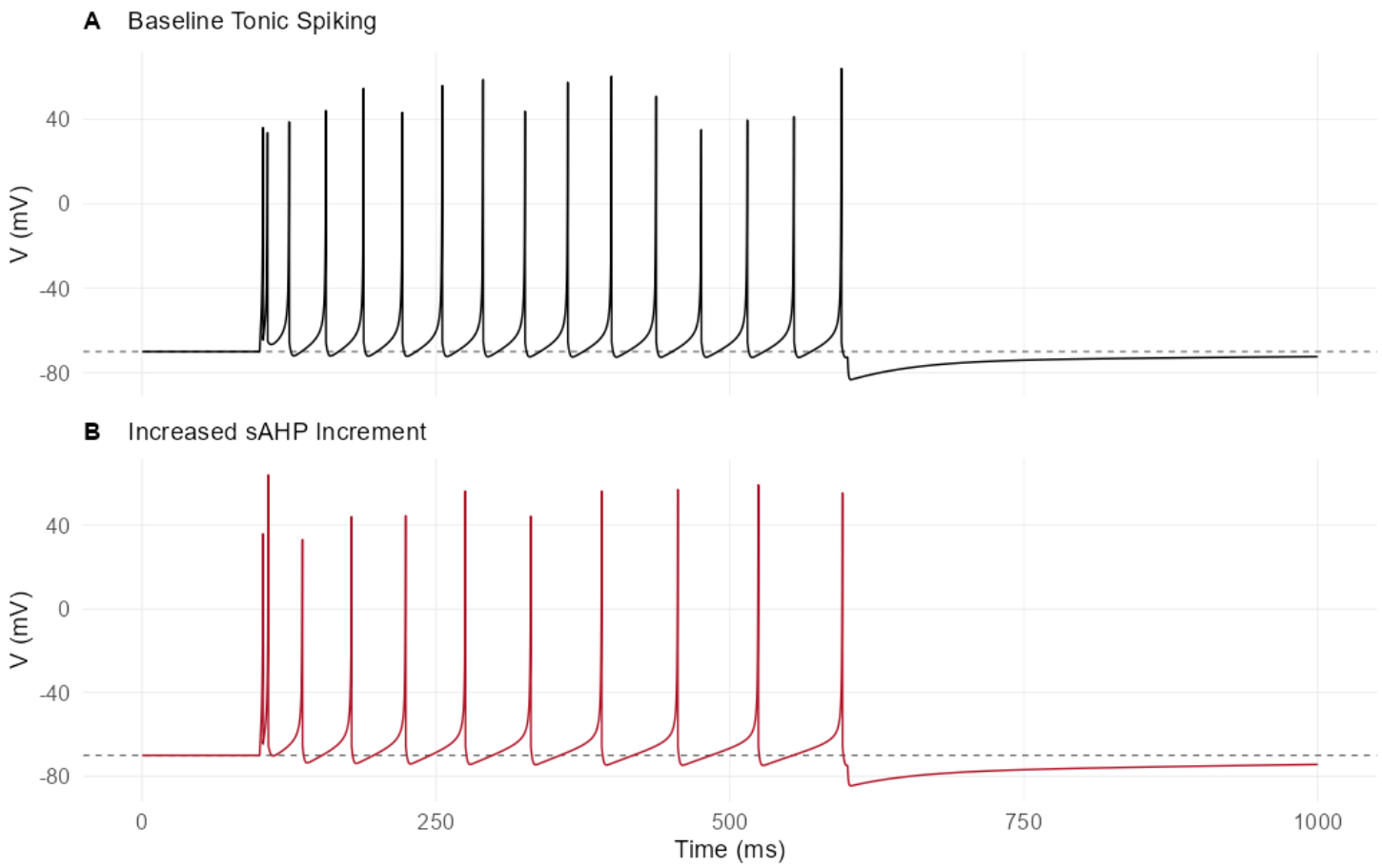


Figure 2

Single-neuron simulations showing how the sAHP modulates firing in an Izhikevich model. Stimulus is applied continuously from 100 to 600 ms. (A) Control neuron without sAHP current applied shows sustained spiking throughout stimulus duration. (B) Application of a stronger sAHP hastens adaptation during stimulation, dramatically reducing spike frequency and producing a more pronounced hyperpolarization once the stimulus is turned off. Both simulations use identical input currents and stimulus durations; sAHP strength is modulated by varying the sAHP decay and increment per spike parameters.

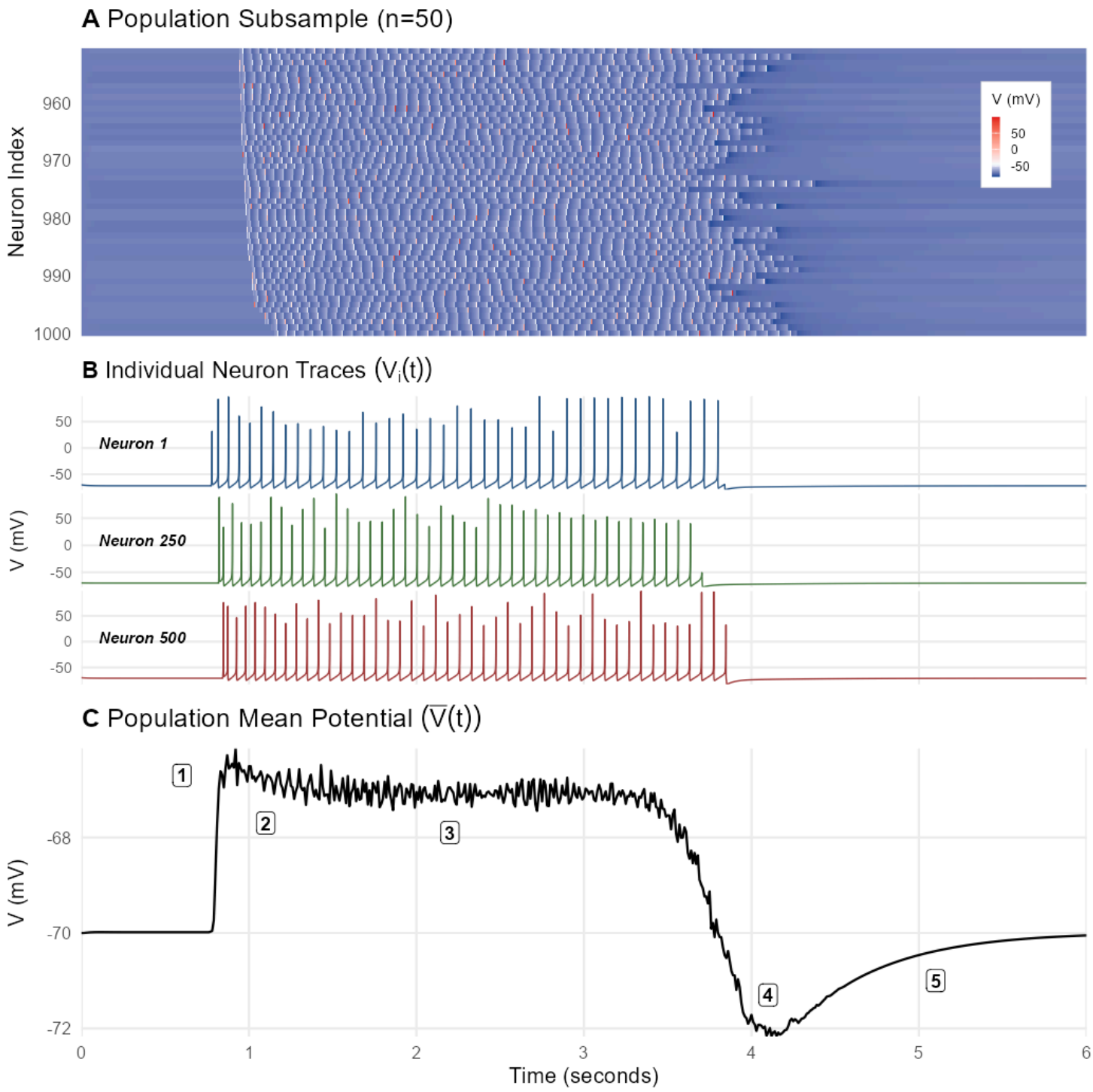


Figure 3

Emergence of the macroscopic affective curve from asynchronous neural activity. (A) Heatmap showing membrane potentials for n=50 neurons with stochastic activation and parameter heterogeneity. (B) Membrane potentials V_i (t) for three individual regular spiking neurons. (C) Macroscopic mean-field potential $\bar{V}(t)$, aggregated across N=1000 neurons, reproducing the SPOAD trace.

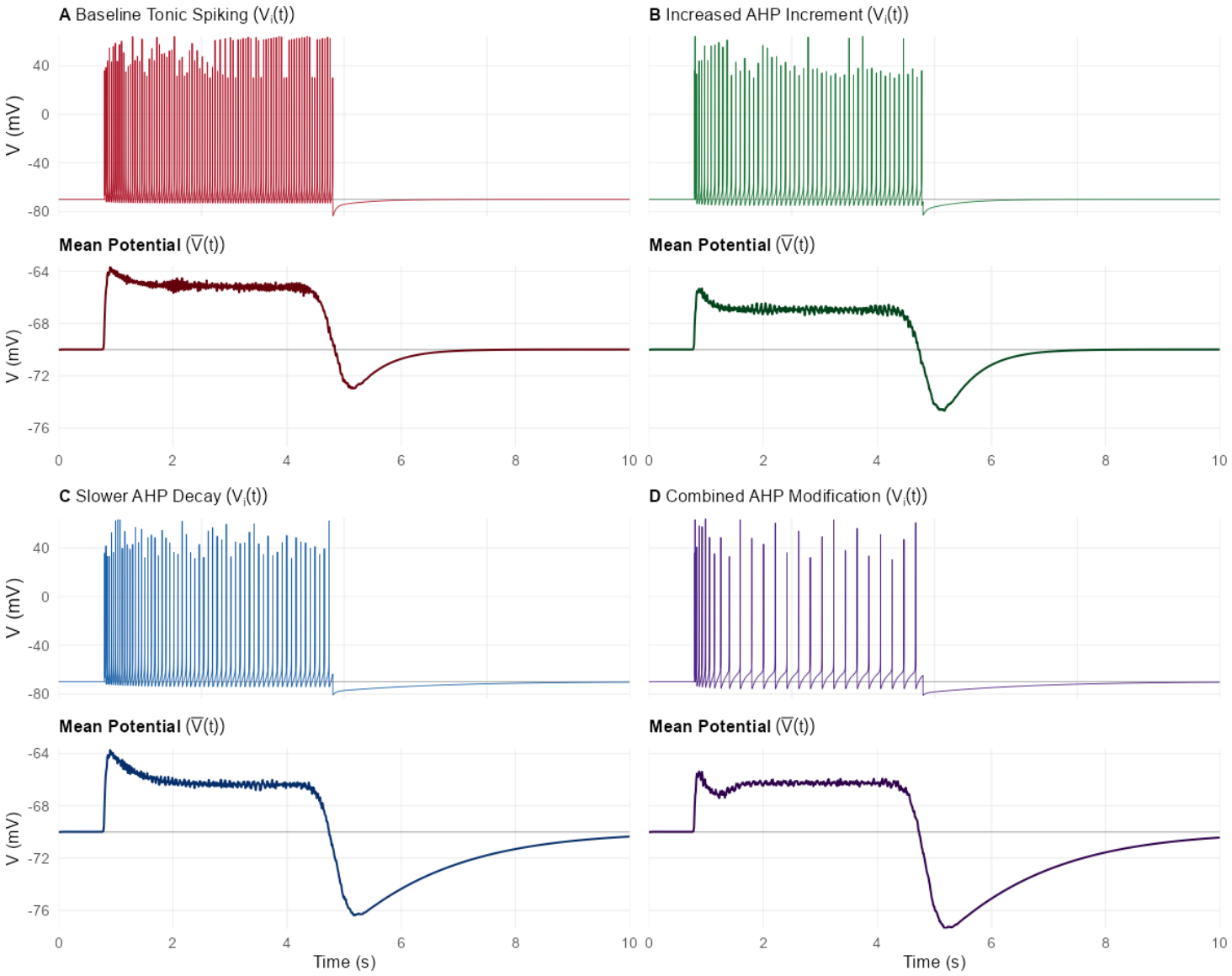


Figure 4

Demonstration of the sAHP's role in shaping opponent-process dynamics following repeated stimuli. Each quadrant shows a single neuron's voltage trace under different sAHP parameter conditions (top) and the corresponding population mean-field potential (bottom) for a population of 1000 BLA neurons. (A) Baseline: A standard tonic-spiking neuron population produces a balanced a- and b-process. (B) Increased sAHP increment: Increasing δ_{AHP} reduces the a-process amplitude and slightly potentiates the b-process. (C) Slower sAHP decay: increasing τ prolongs the decay of the b-process. (D) Combined effect: Increasing both δ_{AHP} and τ dramatically attenuates the a-process while producing an intense and sustained b-process.

Supplementary Files

This is a list of supplementary files associated with this preprint. Click to download.

- SupplementaryMaterials.zip